SUPPORTING INFORMATION

Hierarchical Core–Shell Nanoplatforms Constructed from Fe_3O_4@C and Metal-Organic Frameworks with Excellent Bilirubin Removal Performance

Na Gan, Qiaomei Sun*, Ludan Zhao, Shuangshuang Zhang, Zili Suo, Xinlong Wang*, Hui Li

School of Chemical Engineering, Sichuan University, Chengdu 610065, Sichuan, China

* Corresponding author:

Qiaomei Sun: qiaomeisun@163.com

Xinlong Wang: wangxl@scu.edu.cn

Postal address: School of Chemical Engineering, Sichuan University, Chengdu 610065, China

Contents:

S1. Materials and Characterization

Materials

Bilirubin (99%), Zirconium (IV) chloride (99%), 2-aminoterephthalic acid (BDC-NH_2, 99%), polyvinyl pyrrolidone PVP K30 (99%), ferrocene (98%), N-hydroxysuccinimide (NHS, 98%) and 1-(3-Dimethylaminopropyl)-3-ethylcarbodiimide hydrochloride (EDC, 98%) were purchased from J&K Chemicals (Beijing, China); Analytically pure acetic acid, poly(sodium-p-styrenesulfonate) (PSS), N,N-Dimethylformamide (DMF), dichloromethane, acetone, hydrogen peroxide (30%) and sodium hydroxide (99%) were purchased from KeLong Chem (Chengdu, China); mPEG-NH_2 2000 (97%) was bought from , Albumin bovine serum (BSA, fraction V) was obtained from Caibio Chem (USA); Fetal bovine serum (FBS, qualified) was purchased from Gibco (US); PBS buffer (pH=7.2~7.4), DMEM medium (high glucose) and trypsin-EDTA solution without phenol red were purchased from Sangon Biotech (Shanghai, China); Cell counting kit-8 (CCK-8) was obtained form Meilunbio (Dalian, China); Cells, Caco-2, 293T and LO2 were purchased from Type Culture Collection of the Chinese Academy of Sciences (Shanghai, China); Vacuum blood collection with 3.2% sodium citrate (Weigao, Shandong); Fresh blood, obtained from a healthy adult pig (Laboratory Animal Centre, Sichuan University (Chengdu, China)), all the animal experiments were conducted in compliance with the guidelines for the care and use of laboratory animals from the National Institutes of Health. Ultra-pure water used in this work was made in the laboratory.

Characterization

X-ray diffraction (XRD) was measured on diffractometer (X'Pert PRO; PANalytical, Almelo, Netherlands) with PIXcel 1D detector and Cu Ka radiation. Scanning Electron Microscope (SEM) measurements were performed on JSM-7500F JEOL (Tokyo, Japan) equipped with a field emission gun at 15.0 kV, elemental analysis was conducted on an EDX equipped on the S-4800. Transmission Electron Microscope (TEM) measurements were collected on FEI Talos-F200S. Zeta-potential

measurements were carried out using Zetasizer Nanosizer, Nano ZS (Malvern, Britain). Brunner−Emmet−Teller (BET) measurements were performed on TriStar 3000 Surface Area and Pore Size Analyzer (HOSIC, UK). The content of Zr element was analyzed by Inductively Coupled Plasma Optical Emission Spectrometer (ICP-OES) analysis was carried out on Optima 7000 DV (PerkinElmer, USA). Fourier Transform Infrared Spectrometer (FT-IR) spectra were collected on a Nicolet-6700 FT-IR spectrometer (Thermo, USA) equipped with a smart OMNI-sampler accessory. UV-vis spectra were obtained using a TU1901 double beam UV-vis spectrophotometer (Purkinje General, Beijing, China). Vibrating Sample Magnetometer (VSM) measurements were performed on Lake Shore 7410 (USA). Automatic Coagulation Analyzer (CS-5100, Sysmex, USA). Low speed centrifuge (TB4B, Hunan). High speed centrifuge (5418, Eppendorf, USA).

S2. Material Preparation

Preparation of Fe_3O_4@C

The preparation of Fe_3O_4@C was referred to the literature. 0.3g ferrocene was dissolved in 30mL acetone with ultrasonic dispersion, and then 1.5mL hydrogen peroxide was slowly dropped into the solution. After 10 min of magnetic stirring (300 rpm), precursor solution was placed in a 50mL polytetrafluoroethylene reactor and heated at 200℃ for 24h. After the reaction, the solution was cooled naturally at room temperature, separated by magnetic separation, cleaned with acetone for three times, and then dried in vacuum at 60℃ for 24h.

Preparation of Single with hierarchical pore

To obtain uniform morphology and appropriate size Fe_3O_4@C@Uio66-NH_2 core-shell structure, by changing the reactant: (1) the molar ratio of metal ion and organic ligand; (2) surface negative charge modify reagent, PSS; (3) surfactant, PVP; (4) monobasic acid competition reagent: AcOH, the desired products were successfully prepared (Table S1). Optimization of experimental condition was judged by XRD and SEM of the product (Fig. S2). The exploration process was mainly divided into three

groups: Group A, B and C. In group A, the Bragg peak of MOFs in sample 3 was obvious, which indicated that PSS is helpful to the growth of MOF on Fe_3O_4@C; In group B, PVP and AcOH can make the product more uniform and the crystallinity of MOFs was higher; To obtain the optimal product, this study further changed the molar ratio of reactants in Group C, it can be seen from Fig. S2 that sample 7 has the uniform dispersion and higher crystallinity. Flowing products, Single and Double, were then prepared under this condition.

The preparation method of the final product: 50mg prepared Fe_3O_4@C was dissolved in 10mL DMF with ultrasonic dispersion, and then 150μL PSS modifier was added and shaken at room temperature for 1h (200 rpm); after magnetic separation, it was dispersed into 5mL DMF again, and the 10mL DMF (containing 36mg $ZrCl_4$ + 40mg PVP) was added and shaken for 1h; 15mL DMF (containing 38mg BDC-NH_2) and 1.5mL AcOH were added and shaken for another 0.5h; the precursor solution was reacted in a 50mL polytetrafluoroethylene reactor at 110℃ for 24h, After the reaction, the solution was cooled naturally at room temperature, separated by magnetic separation, cleaned with DMF for three times, and then dried in vacuum at 70℃ for 24h.

To introduce mesoporous in Fe_3O_4@C@Uio66-NH_2 core-shell structure, the volume of AcOH (1.5mL, 4mL, 7mL, i.e. 5%, 15%, 20% (v/v)) was changed in corresponding synthesis process. Name the product Fe_3O_4@C@Uio66-NH_2 prepared under 15% (v/v) AcOH as Single.

Table S1. Synthesis Conditions of Different Products. "+" represents adding the reagent, "√" represents the optimization condition.

Group	Sample	Fe_3O_4@C (mg)	$ZrCl_4$ (mmol)	BDC-NH_2 (mmol)	PSS (150μL)	PVP (40mg)	AcOH (1.5 mL)	Result
A	1	50	0.1	0.1				
	2	50	0.2	0.2				
	3	50	0.1	0.1	+			√
B	4	50	0.1	0.1	+	+		
	5	50	0.1	0.1	+	+	+	√√

	6	50	0.15	0.15	+	+	+	
C	7	50	0.15	0.2	+	+	+	√√√
	8	50	0.15	0.3	+	+	+	

Preparation of Double

50mg Single was dissolved in 10 mL DMF with ultrasonic dispersion, and then 300μL PSS modifier was added and shaken at room temperature for 1h (200 rpm); after magnetic separation, it was dispersed into 5mL DMF again, and the 10mL DMF (containing 36mg $ZrCl_4$ + 40mg PVP) was added and shaken for 1h; 15mL DMF (containing 38mg BDC-NH_2) and 1.5mL AcOH were added and shaken for another 0.5h; the precursor solution was reacted in a 50mL polytetrafluoroethylene reactor at 110℃ for 24h, After the reaction, the solution was cooled naturally at room temperature, separated by magnetic separation, cleaned with DMF for three times, and then dried in vacuum at 70℃ for 24h. Name the product as Double.

Preparation of Double-PEG

50mg Double was dispersed into 10mL ultra-pure water, 50mg EDC, 50mg NHS and 75mg mPEG-NH_2 were dissolved in 5mL ultra-pure water respectively; mix and shake the Double, EDC and NHS solutions for 0.5h (200 rpm), and then add the mPEG-NH_2 solution. The precursor solution reacted at room temperature for 24h under consistent shaking. After the reaction, separated by magnetic separation, cleaned with DMF for three times, and then dried in vacuum at 60℃ for 24h. Name the product as Double-PEG.

Adsorption performance investigation

Bilirubin adsorption of products in PBS and biological solution

All adsorption tests were performed under dark conditions in triplicate. 6mg product was dispersed in 1mL PBS solution; 6.3mg bilirubin was first dissolved in 0.1M NaOH solution in advance and then dispersed in 35mL PBS; 6.3mg bilirubin and

1.68g BSA were together dispersed in 35mL PBS solution; 1.8mg bilirubin was dispersed in 10mL 100% FBS solution; 1.8mg bilirubin was dispersed in 10mL pig's whole blood. 1mL product dispersion was added to 5mL of bilirubin, bilirubin-BSA, bilirubin-FBS and bilirubin-whole blood solutions, respectively (final concentration, product: 1mg mL^{-1}, bilirubin: 150μg mL^{-1}, BSA: 40mg mL^{-1}), shaking at 37℃ (200rpm). At adsorption time 5, 15, 30, 60, 120, 180, 240min, take 50μL of supernatant dispersed in 3mL PBS to measure the absorbance at 438nm (PBS), 460nm (BSA) and 468nm (FBS and whole blood).

Establish bilirubin UV-vis standard curves of different detecting waves in PBS medium at room temperature, as follows:

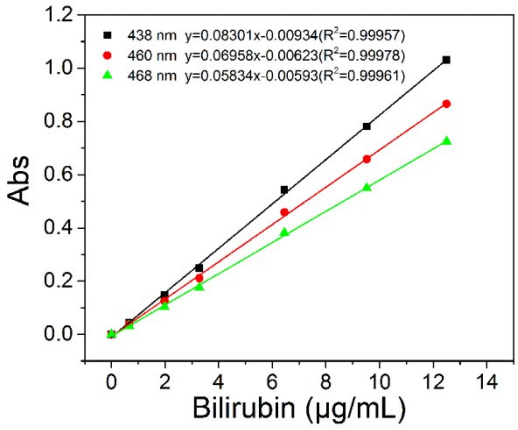

Fig. S1 UV-vis standard curve of bilirubin in PBS solution at 438nm, 460nm and 468nm.

Bilirubin adsorption kinetics of Single and Double-PEG[1,2]

The adsorption date of bilirubin in PBS was selected for kinetic research. The bilirubin uptake at specific time (q_t) and equilibrium (q_e) is obtained by the following formula:

$$q_t = \frac{(C_0 - C_t) \times V}{m} \quad (1)$$

$$q_e = \frac{(C_0 - C_e) \times V}{m} \quad (2)$$

Where q_t and q_e (mg g^{-1}) are the mass of adsorbent adsorbing bilirubin per unit mass

at specific time and equilibrium; C_0, C_t and C_e (mg L^{-1}) are concentration of bilirubin at initial, specific time and equilibrium; V (L) is the solution volume; m (g) is the mass of the adsorbent.

Fit the data with two widely used kinetic models, pseudo-first-order and pseudo-second-order models by the following formula :

Pseudo-first-order model:

$$\ln(q_e - q_t) = lnq_{e,cal,1} - k_1 t \quad (3)$$

Pseudo-second-order model:

$$\frac{t}{q_t} = \frac{1}{k_2 q_{e,cal,2}^2} + \frac{1}{q_{e,cal,2}} \quad (4)$$

Where q_t (mg g^{-1}) and q_e (mg g^{-1}) are the mass of adsorbent adsorbing bilirubin per unit mass at specific time and equilibrium; $q_{e,cal,1}$ (mg g^{-1}) and $q_{e,cal,2}$ (mg g^{-1}) are bilirubin uptake at equilibrium calculated by pseudo-first-order and pseudo-second-order models, respectively; k_1 (min^{-1}) and k_2 (g mg^{-1} min^{-1}) are rate constants calculated by pseudo-first-order and pseudo-second-order models, respectively; $h=k_2 q_{e,cal,2}^2$ is the initial adsorption rate (mg g^{-1} min^{-1}) calculated by the pseudo-second-order model.

Bilirubin adsorption isotherm of Single and Double-PEG[1,3,4]

6mg product was dispersed in 1mL PBS solution; 54mg bilirubin was first dissolved in 0.1M NaOH solution in advance and then dispersed in 30mL PBS; The product was added to the bilirubin solution diluted to 150, 300, 450, 600, 750, 900, 1050, 1200, 1350, 1500 μg mL^{-1} with PBS, shaken for 2h at 37℃ (200 rpm), take 50μL of supernatant dispersed in 3mL PBS to measure the absorbance at 438nm.

Two commonly used fitting models are applied for adsorption isotherm data, Freundlich and Langmuir models:

Nonlinear Freundlich model:

$$q_e = k_F C_e^{\frac{1}{n}} \quad (5)$$

Linear Freundlich model:

$$\ln\left(q_e\right) = \frac{1}{n}\ln\left(C_e\right) + ln(k_F) \tag{6}$$

Nonlinear Langmuir model:

$$q_e \frac{q_m k_L C_e}{1 + k_L C_e} \tag{7}$$

Linear Langmuir model:

$$\frac{1}{q_e} = \frac{1}{q_m k_L C_e} + \frac{1}{q_m} \tag{8}$$

Separation factor of Langmuir isotherm:

$$R_L = \frac{1}{1 + k_L C_0} \tag{9}$$

Where q_e is the bilirubin uptake at equilibrium; k_F((mg g^{-1})(L mg^{-1})$^{1/n}$) is Freundlich constant; 1/n is the Freundlich exponent; C_0 and C_e are the initial and equilibrium concentration of bilirubin. q_m (mg g^{-1}) is the maximum adsorption capacity fitted by the Langmuir model; K_L (L mg^{-1}) is the Langmuir constant； R_L is the separation factor， when $R_L = 0$, $0 < R_L < 1$, $R_L = 1$, or $R_L > 1$, the adsorption tend to be irreversible, favorable, linear, or unfavorable, respectively.

Cytotoxicity test[5]

Cells were cultured in the environment of 37 °C and 5% CO_2 in DMEM, supplemented with 10% FBS, 100 U/mL penicillin and 100 μg/mL streptomycin.

The samples were dispersed and diluted with PBS solution. Select human embryonic kidney cell (293T), human normal hepatocytes (LO2) and human colorectal adenocarcinoma cells (Caco2) to investigate the cytotoxicity of the products Single, Double and Double-PEG by CCK-8 method. Approximately 1×10^5 cells were added to 96-well plate, after 24h of incubation, adding product with final concentration of 20, 50, 100 μg mL^{-1}. After another 24h of incubation, add 10μL CCK-8 reagent and continue to incubate for 2h in the incubator. Absorbance at 450nm was collected using a microplate reader (Molecular Devices, USA).

Cell survival rate was calculated as follows:

$$\text{Cell survival rate\%} = (OD_{exp} - OD_{bla}) / (OD_{neg} - OD_{bla}) \times 100\% \tag{10}$$

The OD_{exp} is the absorbance value of the experimental group; the OD_{neg} is the

absorbance value of the negative control group with only cells; the OD_{bla} is the blank control group without cells. The safe concentration is the concentration corresponding to the cell survival rate ≥ 90%.

Hemolysis test[6]

5 mL fresh EDTA anticoagulated pig blood was added to 10 mL saline to centrifuged at 1500rpm for 5min , and the precipitated layer was washed five times with saline to obtain the red blood cells. The red blood cells were resuspended with a concentration of 20% in saline. 0.3mL red blood suspension was immersed in 1.2 mL saline and deionized water used as the negative and positive control, respectively; 0.3mL red blood suspension was immersed in 1.2 mL Fe_3O_4@C, Single, Double and Double-PEG samples with a final concentration of 500μg mL^{-1}. Then the mixture solutions incubated for 2h at 37°C.

After interaction, the mixture was centrifuged for 5min at 8000 rpm, the solution was observed by a digital camera. The absorbance of centrifuged supernatant was measured at 541nm to calculate the hemolysis ratio with the following formula:

$$Hemolysis\ ratio\ (\%) = \frac{AS - AN}{AP - AN} \tag{11}$$

Where AS is the absorbance of the samples; AN and AP are the absorbance of negative and positive control, respectively.

Anticoagulation tests[16]

After centrifugation for 10 min at 1200×g, the upper layer of anemia platelets plasma (PPP) was obtained. PPP was added into a 15 ml centrifuge tube and mixed upside down; The 450 μL PPP was added into a 1.5 ml centrifuge tube, and then 50 μL of samples were added (the final concentration of the samples was 500 μg / mL), and incubated at 37 ℃ for 60 min. The 450 μL PPP was added with 50μL normal saline as blank control. Three parallel tests were set for each sample. After centrifugation for 5 min at 1200×g, the black brown powder sample was precipitated to the bottom of the centrifuge tube, and the upper plasma was absorbed and added into the new centrifuge tube. The APTT, PT, TT and FIB values were detected by automatic coagulation

analyzer. The batch number of APTT, PT, TT and FIB reagents (Siemens, Germany) is 10445711.

Statistical analysis

All assays were conducted in triplicate. The maximum experimental error in the measurements was 5% and the mean values, standard deviations, and statistical differences were estimated using analysis of variance. Data processing and analyses were performed using the OriginPro software (OriginLab Corporation, Northampton, MA).

S3. Supplementary Fig. S2~S15 and Tables S2~S4

Table S2. Comparison of Equilibrium Uptake and Equilibrium Time in Free bilirubin and BSA Solution for Double-PEG with Other Adsorption Materials

Type	Materials	Free bilirubin		BSA bilirubin			Year	Ref
		q_e (mg g^{-1})	T (min)	[C] (mg mL^{-1})	q_e (mg g^{-1})	T (min)		
AC	AC	----	----		0.24	120	2017	[7]
	Dextran-coated AC	----	----	----	7.4	120	2016	[8]
	Zwitterionic hydrogel coated AC	----	----	----	8.0	120	2017	[7]
Magnetic materials	Magnetic multiwalled carbon nanotubes	263.16	150	----	----	----	2012	[9]
	Carbon nanotubes/magnetite/chitin magnetic nanocomposite	6.19	20	----	----	----	2014	[10]
	Magnetic nitrogen-doped porous carbon	----	----	40	72.4	115	2017	[11]
Composite materials	Chitosan/graphene oxide composite aerogel microspheres	178.25	120	----	----	----	2020	[12]
	Organic hec nanocomposites modified with lysine	84.17	180	----	----	----	2019	[13]
	Lysine-immobilized chitin/carbon nanotube microspheres	----	----	10	107.2	180	2017	[3]
Membrane materials	Polyethylenimine grafted electrospun polyacrylonitrile fiber membrane	194.17	180	50	112.87	300	2018	[14]
	Poly(tetrafluoroethylene) membrane	----	----	----	94.5	50	2005	[15]
	Alginate/HSA double-sided functional PVDF multifunctional composite	----	----	20	32.72	180	2020	[16]
	Macro-mesoporous reduced graphene aerogel beads	1361.51	480	40	252.4	480	2020	[17]

	S/L=0.29						
Beads	Chitosan/SiO 2 -loaded graphene composite beads						
	202.39	60	40 S/L=2.3	40	120	2020	[18]
	Carrageenan-Based Heparin-Mimetic Gel Beads						
	228.16	600	----	----	----	2018	[5]
	Graphene oxide based core @ polyethersulfone-based shell beads						
	74.07	240	----	----	----	2020	[19]
	Chitin/graphene oxide composite aerogel beads						
	418.4	90	----	----	----	2019	[20]
	Nano-CaCO3/polystyrene nanocomposite beads						
	----	----	15	24.98	120	2018	[4]
Carbon	Polydopamine decorated ordered mesoporous carbon						
	513.54	30	40 S/L=1.0	122.7	30	2020	[21]
	Hierarchically macro/mesoporous carbon						
	885	120	plasma	10.8	120	2014	[22]
MOFs	PCN-333 and MOF-808						
	1003.8	5	40 S/L=0.2	165.6	30	2020	[1]
	PCB-MIL101 and MIL-101(Cr) based anti-biofouling						
	583	60	40	102.8	180	2020	[2]
Imprinted materials	Bilirubin imprinted polydopamine coated poly(ether sulfone)						
	184.24	120	----	----	----	2017	[23]
Hierarchically Fe_3O_4@NMOFs	1738.29	5	40 S/L=0.2	145.16	60	This work	

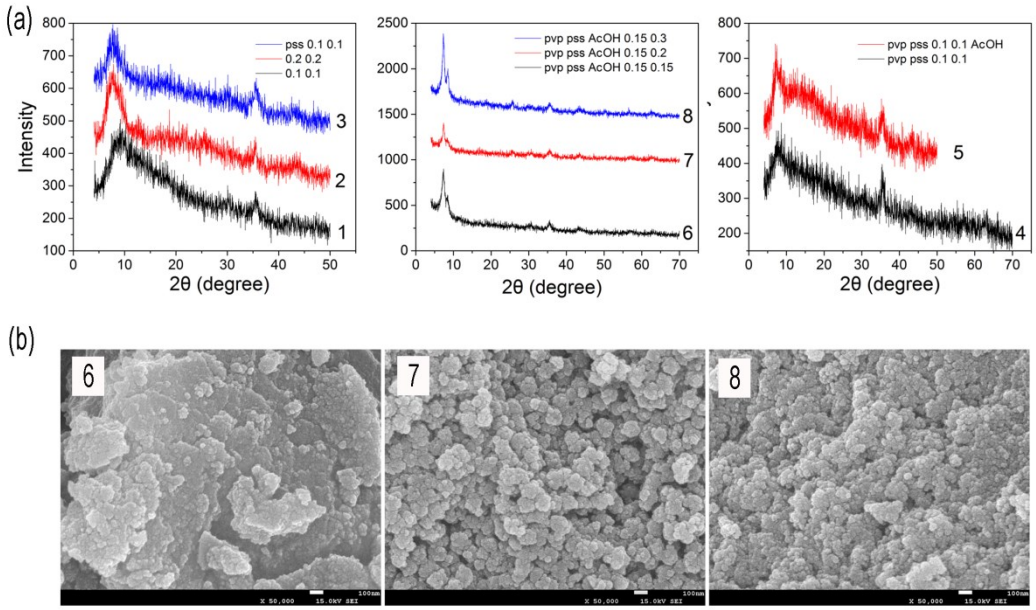

Fig. S2 (a) X-ray diffraction pattern of samples 1~8. (b) SEM mapping pattern of samples 6~8.

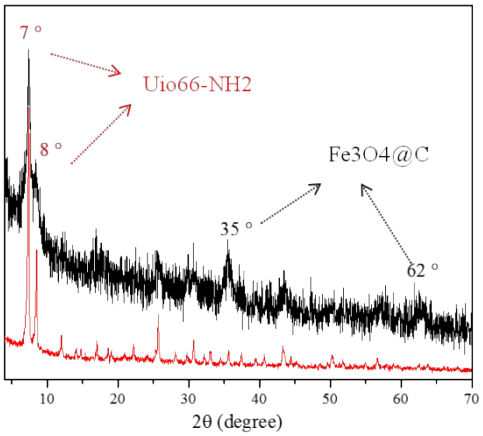

Fig. S3 X-ray diffraction pattern of Fe_3O_4@C and Uio66-NH_2.

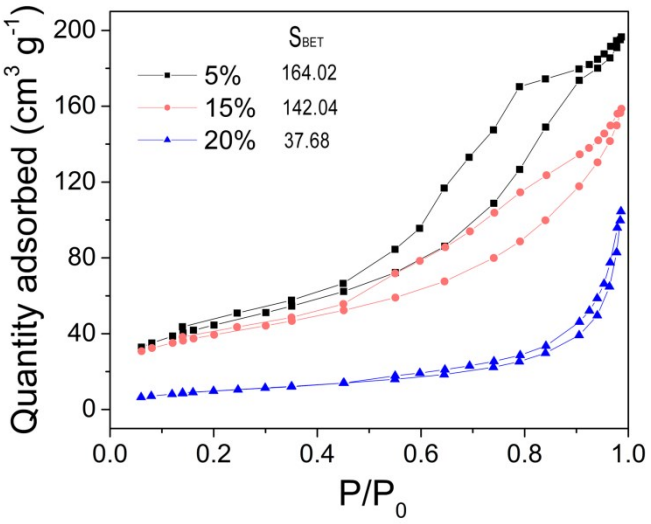

Fig. S4 N_2 adsorption–desorption isotherms patterns of product under different acetic acid volume ratios calculated by Brunauer−Emmett−Teller (BET) method.

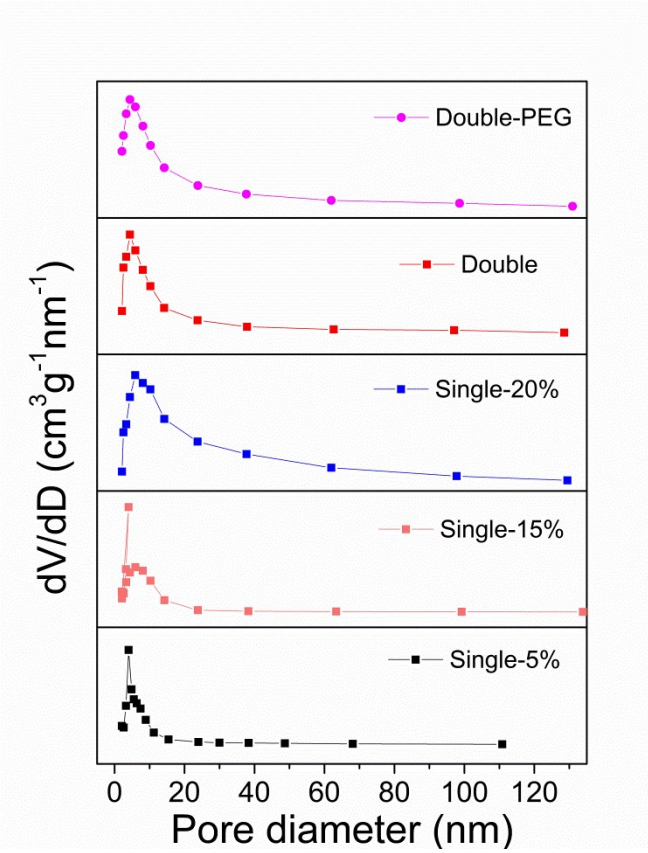

Fig. S5 Pore size distribution calculated by the Barrett−Joyner−Halenda (BJH) method.

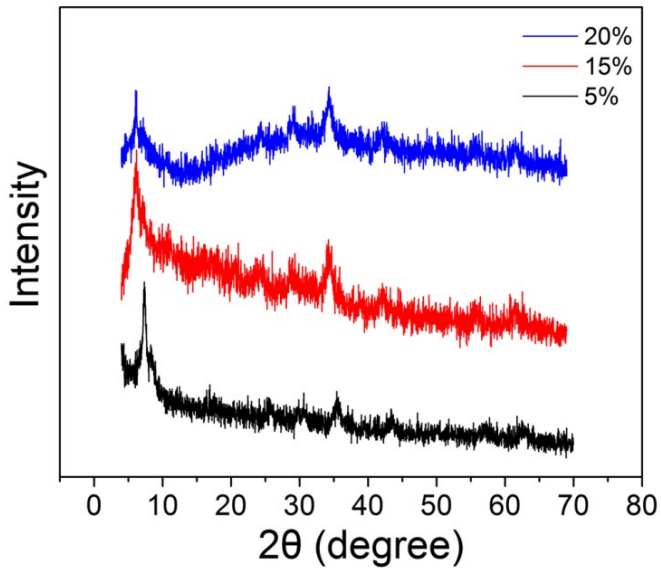

Fig. S6 X-ray diffraction pattern of of product under different acetic acid volume ratio.

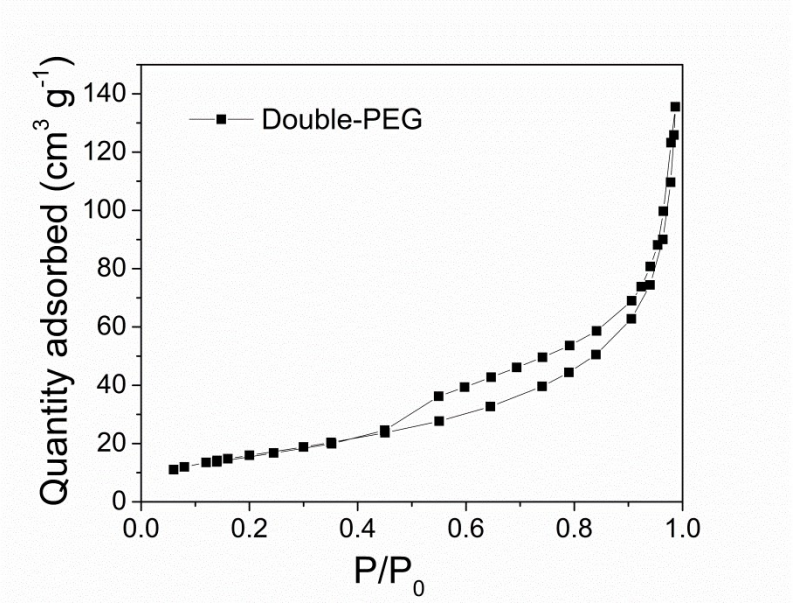

Fig. S7 N_2 adsorption–desorption isotherms patterns of product Double-PEG calculated by Brunauer−Emmett−Teller (BET) method.

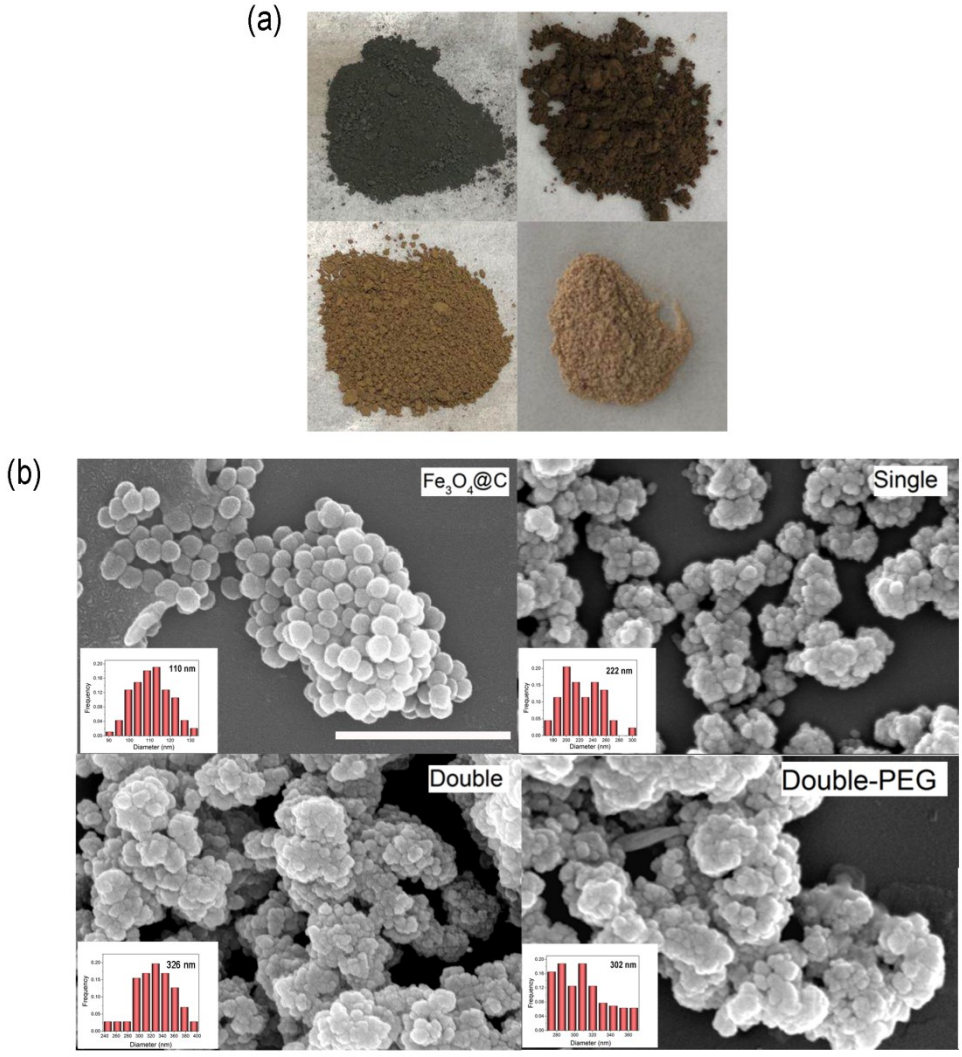

Fig. S8 (a) Electronic photos, (b) SEM mapping pattern of Fe_3O_4@C, Single, Double and Double-PEG, inset: diameter distribution (scale bar: 1μm).

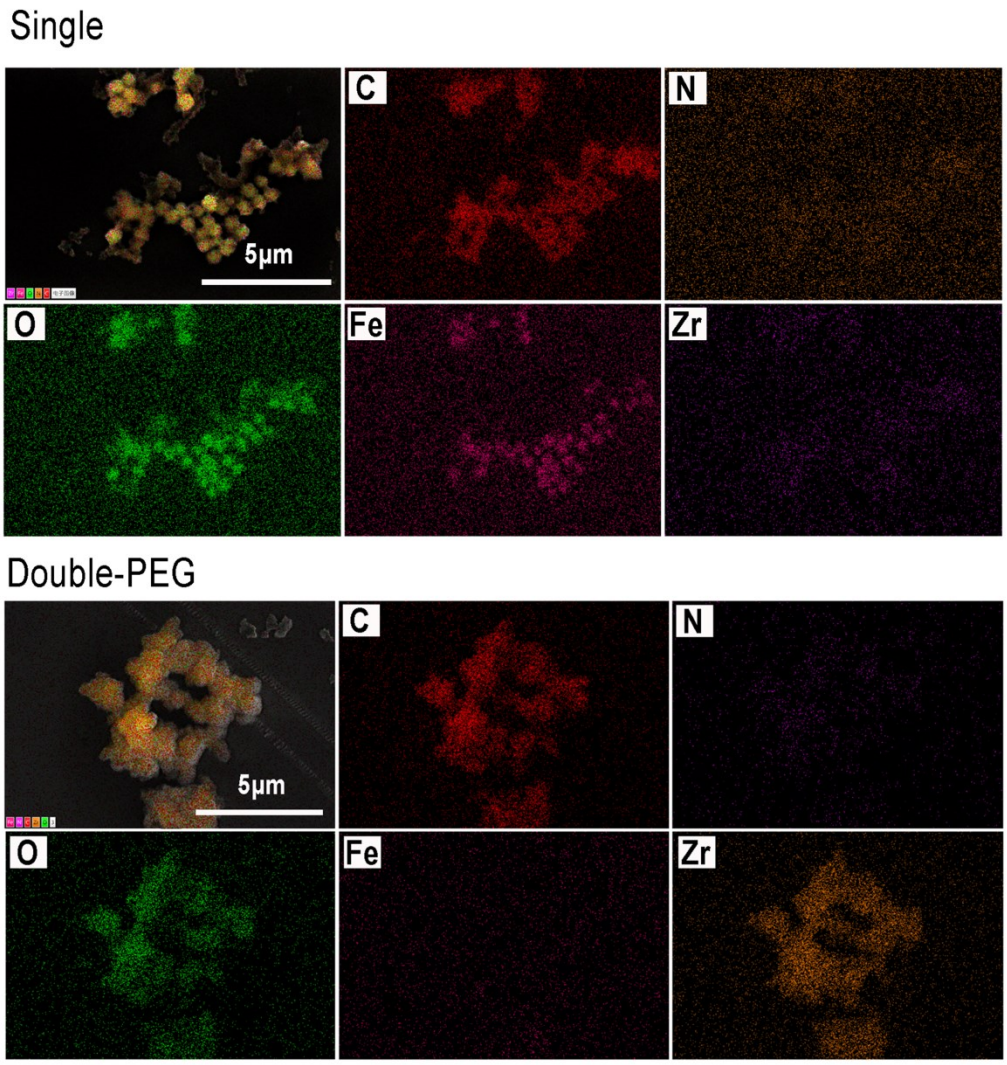

Fig. S9 SEM mapping patterns of Single and Double-PEG.

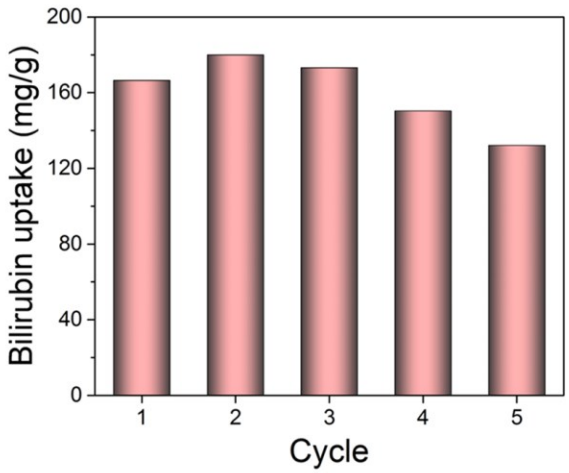

Fig. S10 Regeneration performance of product toward bilirubin uptake.

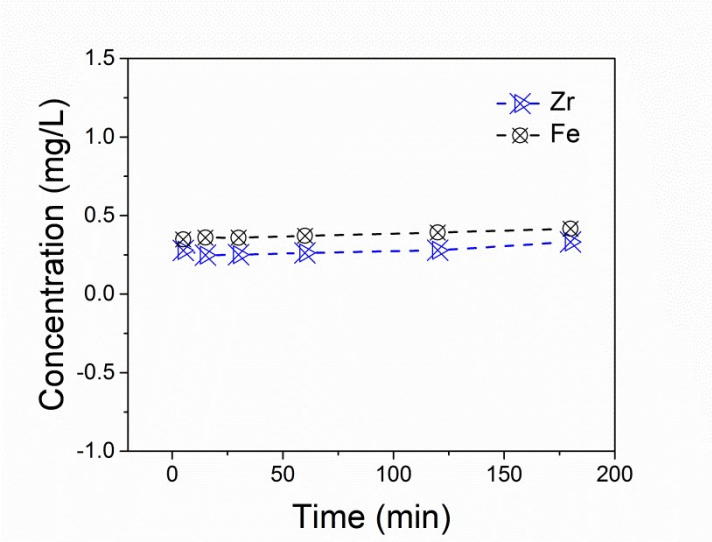

Fig. S11 The concentration of Zr and Fe atoms versus time in 100% FBS solution characterized by ICP-OES.

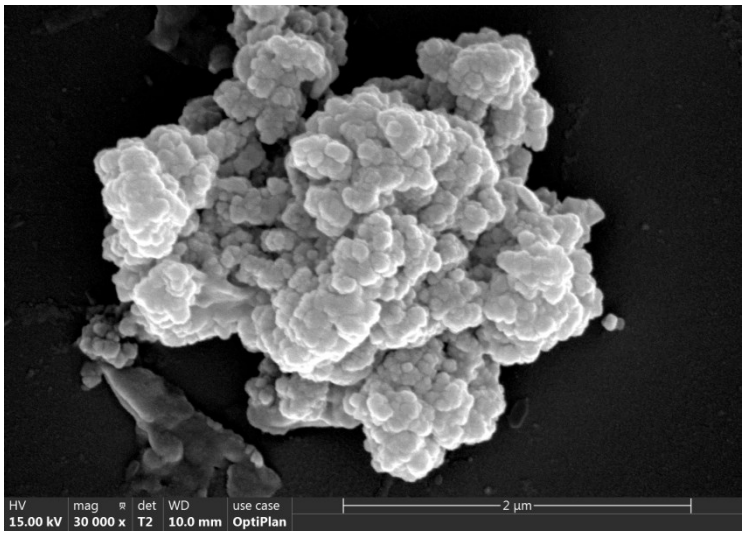

Fig. S12 SEM pattern of Double-PEG after adsorption in 100% FBS solution.

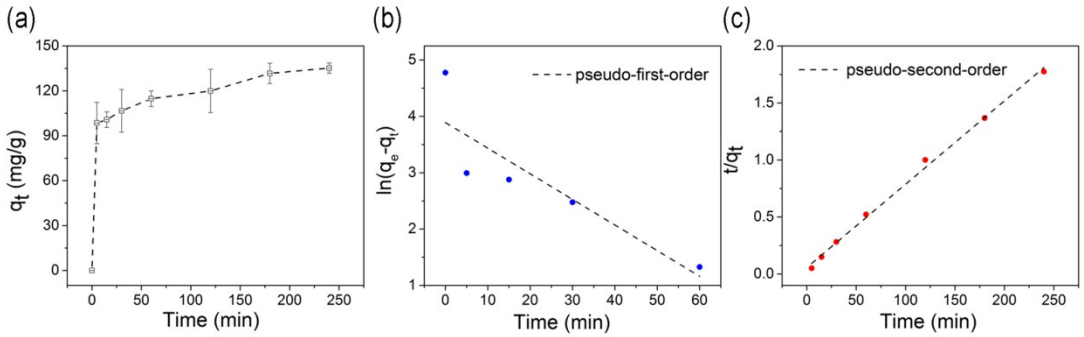

Fig. S13 Bilirubin adsorption kinetics of Sibgle. (a) Bilirubin uptake versus time in PBS solution. Adsorption kinetic: (b) pseudo-first-order and (c) pseudo-second-order fitting plots for bilirubin adsorption.

Table S3. Adsorption Kinetic Parameters of Single toward Free Bilirubin.

pseudo-first-order		
$q_{e,cal,1}$ (mg g^{-1})	k_1 (min^{-1})	R^2
48.92	0.0155	0.7051
pseudo-second-order		
$q_{e,cal,2}$ (mg g^{-1})	k_2 (g $mg^{-1}min^{-1}$)	h (mg g^{-1} min^{-1})	R^2
122.10	0.0028	41.14	0.9998

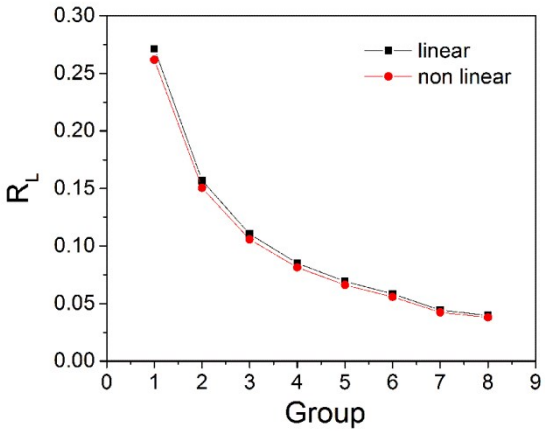

Fig. S14 Separation factor (R_L) in the Langmuir model fitting results.

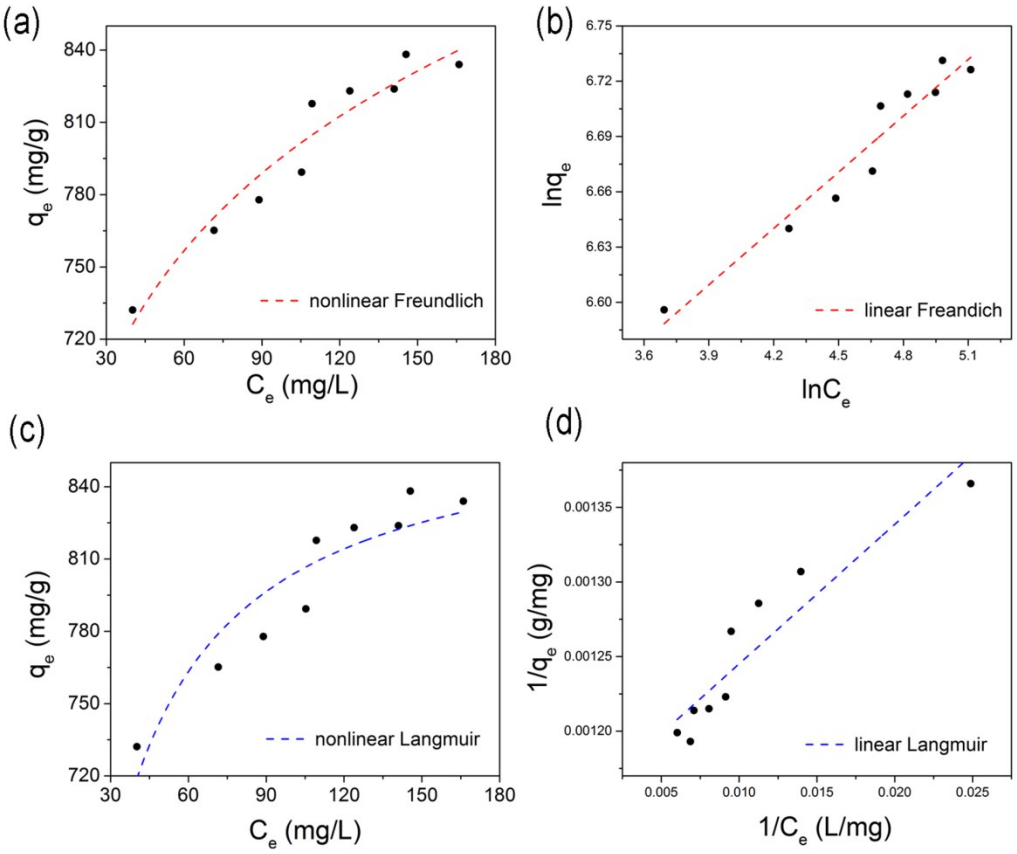

Fig. S15 Bilirubin adsorption isotherms in PBS solution of Single: (a,b) nonlinear Freundlich and linear Freundlich, (c,d) nonlinear Langmuir and linear Langmuir model fitting plots.

Table S4. Adsorption Isotherm Parameters of Single toward Free Bilirubin.

Langmuir			
fitting method	q_m (mg g^{-1})	K_L (L mg^{-1})	R^2
linear	869.57	0.123	0.8560
non linear	872.43	0.117	0.8536
Freandich			
fitting method	k_F (mg g^{-1}) (L mg^{-1})$^{1/n}$	1/n	R^2
linear	498.80	0.102	0.9388
non linear	497.22	0.103	0.9262

S4. References

[1] Q. Li, W. Zhao, H. Guo, J. Yang, J. Zhang, M. Liu, T. Xu, Y. Chen, L. Zhang, *ACS Appl. Mater. Inter.,* 2020, **12,** 25546-25556.

[2] Q. Li, H. Guo, J. Yang, W. Zhao, Y. Zhu, X. Sui, T. Xu, J. Zhang, L. Zhang, *Langmuir,* 2020, **36,** 8753–8763.

[3] S. Wu, B. Duan, X. Zeng, A. Lu, X. Xu, Y. Wang, Q. Ye, L. Zhang, *J. Mater. Chem. B,* 2017, **5,** 2952-2963.

[4] J. Chen, G. Cheng, Y. Chai, W. Han, W. Zong, J. Chen, C. Li, W. Wang, L. Ou, Y. Yu, *Colloid. Surface. B,* 2018, **161,** 480-487.

[5] X. Song, K. Wang, C.Q. Tang, W.W. Yang, W.F. Zhao, C.S. Zhao, *Biomacromolecules,* 2018, **19,** 1966-1978.

[6] Y. Zhou, B. Yang, X. Ren, Z. Liu, Z. Deng, L. Chen, Y. Deng, L.M. Zhang, L. Yang, *Biomaterials,* 2012, **33,** 4731-40.

[7] N. Cai, Q. Li, J. Zhang, T. Xu, W. Zhao, J. Yang, L. Zhang, *J. Colloid Inter. Sci.,* 2017, **503,** 168-177.

[8] C.A. Howell, S.R. Sandeman, Y. Zheng, S.V. Mikhalovsky, V.G. Nikolaev, L.A. Sakhno, E.A. Snezhkova, *Carbon,* 2016, **97,** 134-146.

[9] H. Wei, L. Xu, J. Ren, L. Jia, *Colloid. Surface. A,* 2012, **405,** 38-44.

[10] M.A. Salam, R.M. El-Shishtawy, A.Y. Obaid, *J. Ind. Eng. Chem.,* 2014, **20,** 3559-3567.

[11] C.F. Ma, Q. Gao, J. Zhou, Q.X. Chen, B. Han, K.S. Xia, C.G. Zhou, *RSC Adv.,* 2017, **7,** 2081-2091.

[12] K. Wu, X. Liu, Z. Li, Y. Jiao, C. Zhou, *Mat. Sci. Eng. C,* 2020, **106,** 110162.

[13] C. Li, W. Zhang, N. Yang, Q.S. Zhang, *Appl. Biochem. Biotech.,* 2019, **188,** 769-786.

[14] R. Zhao, Y. Li, X. Li, Y. Li, B. Sun, S. Chao, C. Wang, *J. Mater. Chem. A,* 2017, **5,** 1133-1144.

[15] L. Zhang, G. Jin, *J. Chromatog. B,* 2005, **821,** 112-121.

[16] J. Liu, G. Shu, X. Lu, K. Li, X. Kong, S. Zheng, R. Ma. T. Li, *Sep. Purif. Technol.,* 2020, **252,** 117295.

[17] Z. Li, X. Huang, K. Wu, Y. Jiao, C. Zhou, *Mat. Sci. Eng. C,* 2020, **106,** 110282.

[18] J. Chen, Y. Ma, L. Wang, W. Han, Y. Chai, T. Wang, J. Li, L. Ou, *Carbon,* 2019, **143,** 352-361.

[19] C. He, M. Li, J. Zhang, B. Yan, W. Zhao, S. Sun, C. Zhao, *Macromol. Biosci.,* 2020, **20,** e2000153.

[20] X. Song, X. Huang, Z. Li, K. Wu, Y. Jiao, C. Zhou, *Carbohyd. Polym.,* 2019, **207,** 704-712.

[21] S. Huang, J. Zheng, Y. Zhang, J. Zheng, Z. Zhuang, Q. Yang, F. Wang, G. Chen, S. Huang, G. Ouyang, *J. Mater. Chem. B,* 2020, **8,** 290-297.

[22] G. Tao, L. Zhang, Z. Hua, Y. Chen, L. Guo, J. Zhang, Z. Shu, J. Gao, H. Chen, W. Wu, Z. Liu, J. Shi, *Carbon,* 2014, **66,** 547-559.

[23] K. Wu, W. Yang, Y. Jiao, C. Zhou, *J. Mater. Chem. B,* 2017, **5,** 5763-5773.